Supervisory Predictive Control of Standalone Wind/Solar Energy Generation Systems

Wei Qi, Jinfeng Liu, Xianzhong Chen, and Panagiotis D. Christofides, *Fellow, IEEE*

***Abstract*—This work focuses on the development of a supervisory model predictive control method for the optimal management and operation of hybrid standalone wind-solar energy generation systems. We design the supervisory control system via model predictive control which computes the power references for the wind and solar subsystems at each sampling time while minimizing a suitable cost function. The power references are sent to two local controllers which drive the two subsystems to the requested power references. We discuss how to incorporate practical considerations, for example, how to extend the life time of the equipment by reducing the peak values of inrush or surge currents, into the formulation of the model predictive control optimization problem. We present several simulation case studies that demonstrate the applicability and effectiveness of the proposed supervisory predictive control architecture.**

***Index Terms*—Model predictive control (MPC), solar energy, standalone wind and solar systems, supervisory predictive control, wind energy.**

I. Introduction

ALTERNATIVE energy technologies, like wind- and solar-based energy generation systems, are receiving national and worldwide attention owing to the rising rate of consumption of nuclear and fossil fuels. In particular, drivers for solar/wind renewable energy systems are the environmental benefits (reduction of carbon emissions due to the use of renewable energy sources and the efficient use of fossil fuels), reduced investment risk, fuel diversification, and energy autonomy, increased energy efficiency (less line losses) as well as potential increase of power quality and reliability and in certain cases, potential grid expansion deferral due to the possibility of generation close to demand. In a recent report of the California Energy Commission, for example, the state's target is to generate from renewable sources the 33% of the energy needed by year 2020, with about 70% of that energy being produced by wind and solar systems [1]; many other states have similar goals. However, achieving such major renewable energy production goals requires addressing key fundamental challenges in the operation and reliability of intermittent (variable output) renewable resources like solar- and wind-based energy generation systems. Specifically, unexpected drops in energy production of a solar or wind energy system may require quick start units to cover the shortfall while unexpected increases require the ability to absorb the unscheduled generation. One way to deal with the variable output of wind and solar energy generation systems is through the use of integrated energy generation systems using both wind and photovoltaic energy, which are also tightly integrated with distributed energy storage systems (batteries) and controllable energy loads like, for example, a water production system that operates at controllable time intervals to meet specific demand.

With respect to previous results on control of wind and solar systems, most of the efforts have focused on standalone wind or solar systems. Specifically, there is a significant body of literature dealing with control of wind energy generation systems (see, for example, [2]–[12] for results and references in this area), while several contributions have been made to the control of solar-based energy generation systems (see, for example, [13]–[17]). However, there are few works that have focused on the control of standalone hybrid wind-solar energy generation systems. In [18], a reduced-order nonlinear model was used to design a controller to regulate the wind power generation to complement the power generated by a photovoltaic subsystem and to satisfy a specific power demand. In [19], sliding mode control techniques were used to control the power generated by a photovoltaic array in order to satisfy the total instantaneous power demand in a highly uncertain operating environment. In [20], a supervisory control system was developed to satisfy the load power demand and to maintain the state of charge of the battery bank to prevent blackout. In a recent work [21], a cost-effective control technique was proposed for maximum power point tracking from the photovoltaic array and wind turbine under varying climatic conditions without measuring the irradiance of the photovoltaic or the wind speed. However, no attention has been given to the development of supervisory control systems for standalone hybrid wind-solar energy generation systems that take into account optimal allocation of generation assignment between the two subsystems.

The objective of the present work is to develop a supervisory predictive control method for the optimal management and operation of hybrid wind-solar energy systems. We propose to design the supervisory control system via model predictive control (MPC) which computes the power references for the wind and solar subsystems at each sampling time while minimizing a suitable cost function. The power references are sent to two local controllers which drive the wind and solar subsystems to the desired power reference values. MPC is a popular control strategy

Manuscript received September 11, 2009; revised December 04, 2009 and January 18, 2010. Manuscript received in final form January 25, 2010. First published February 25, 2010; current version published December 22, 2010. Recommended by Associate Editor J. Lee.

W. Qi, J. Liu, and X. Chen are with the Department of Chemical and Biomolecular Engineering, University of California, Los Angeles, CA 90095-1592, USA (e-mail: qiwei.0216@gmail.com; jinfeng@ucla.edu; xianzhongchen@gmail.com).

P. D. Christofides is with the Department of Chemical and Biomolecular Engineering and the Department of Electrical Engineering, University of California, Los Angeles, CA 90095-1592, USA (e-mail: pdc@seas.ucla.edu).

Color versions of one or more of the figures in this paper are available online at http://ieeexplore.ieee.org.

Digital Object Identifier 10.1109/TCST.2010.2041930

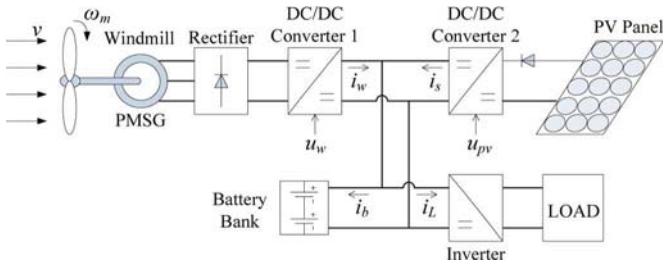

Fig. 1. Wind-solar energy generation system.

because of its ability to account for state and input constraints as well as optimality considerations explicitly in the evaluation of control actions. MPC uses a model of the system to predict at each sampling time the future evolution of the system from the current state along a given prediction horizon [22], [23]. Using these predictions, the input/set-point trajectory that minimizes a given performance index over a finite-time horizon is computed solving a suitable optimization problem subject to constraints. In this work, we discuss how we can incorporate practical considerations (for example, how to extend the life time of the equipments by reducing the peak values of inrush or surge currents) into the formulation of the MPC optimization problem by determining an appropriate cost function and constraints. We present several simulation case studies that demonstrate the applicability and effectiveness of the proposed supervisory predictive control architecture.

II. Wind-Solar System Description

The wind-solar energy generation system considered in this work is based on the models developed in [18]–[20]. A schematic of the system is shown in Fig. 1. In this hybrid system, there are three subsystems: wind subsystem, solar subsystem, and a lead-acid battery bank which is used to overcome periods of scarce generation.

First, we describe the modeling of the wind subsystem. In the wind generation subsystem, there is a windmill, a multipolar permanent-magnet synchronous generator (PMSG), a rectifier, and a dc/dc converter to interface the generator with the dc bus. The converter is used to control indirectly the operating point of the wind turbine (and consequently its power generation) by commanding the voltage on the PMSG terminals.

The mathematical description of the wind subsystem written in a rotor reference frame is as follows [18]:

$$\begin{aligned}
\dot{i}_q &= -\frac{R_s}{L}i_q - \omega_e i_d + \frac{\omega_e \phi_m}{L} - \frac{\pi v_b i_q u_w}{3\sqrt{3}L\sqrt{i_q^2+i_d^2}} \\
\dot{i}_d &= -\frac{R_s}{L}i_d - \omega_e i_q - \frac{\pi v_b i_d u_w}{3\sqrt{3}L\sqrt{i_q^2+i_d^2}} \\
\dot{\omega}_e &= \frac{P}{2J}\left(T_t - \frac{3}{2}\frac{P}{2}\phi_m i_q\right)
\end{aligned} \tag{1}$$

where i_q and i_d are the quadrature current and the direct current in the rotor reference frame, respectively; R_s and L are the per phase resistance and inductance of the stator windings, respectively; ω_e is the electrical angular speed; ϕ_m is the flux linked by the stator windings; v_b is the voltage on the battery bank terminals; u_w is the control signal [duty cycle of the dc/dc converter (dc/dc converter 1 in Fig. 1)], P is the PMSG number of poles, J is the inertial of the rotating parts, and T_t is the wind turbine torque. The wind turbine torque can be written as

$$T_t = \frac{1}{2}C_t(\lambda)\rho A R v^2 \tag{2}$$

where ρ is the air density, A is the turbine-swept area, R is the turbine radius, v is the wind speed, and $C_t(\lambda)$ is a nonlinear torque coefficient which depends on the tip speed ratio ($\lambda = R\omega_m/v$ with $\omega_m = 2\omega_e/P$ being the angular shaft speed).

Based on (1), we can express the power generated by the wind subsystem and injected into the dc bus as follows:

$$P_w = \frac{\pi v_b}{2\sqrt{3}}\sqrt{i_q^2+i_d^2}\,u_w. \tag{3}$$

The model of the wind subsystem can be rewritten in the following compact form:

$$\dot{x}_w = f_w(x_w) + g_w(x_w)u_w \tag{4}$$

where $x_w = [i_q\ i_d\ \omega_w]^T$ is the state vector of the wind subsystem and $f_w = [f_{w1}\ f_{w2}\ f_{w3}]^T$, $g_w = [g_{w1}\ g_{w2}\ g_{w3}]^T$ are nonlinear vector functions whose explicit form is omitted for brevity.

Next, we describe the modeling of the solar subsystem. In the solar subsystem, there is a photo-voltaic (PV) panel array and a half-bridge buck dc/dc converter. The solar subsystem is connected to the dc bus via the dc/dc converter. In this subsystem, similar to the wind subsystem, the converter is used to control the operating point of the PV panels.

The mathematic description of the solar subsystem is as follows [19]:

$$\begin{aligned}
\dot{v}_{\rm pv} &= \frac{i_{\rm pv}}{C} - \frac{i_s}{C}u_{\rm pv} \\
\dot{i}_s &= -\frac{v_b}{L_c} + \frac{v_{\rm pv}}{L_c}u_{\rm pv} \\
i_{\rm pv} &= n_p I_{ph} - n_p I_{rs}\left(\exp\left(\frac{q(v_{\rm pv}+i_{\rm pv}R_s)}{n_s A_c K T}\right) - 1\right)
\end{aligned} \tag{5}$$

where $v_{\rm pv}$ is the voltage level on the PV panel array terminals, i_s is the current injected into the dc bus, C and L_c are electrical parameters of the buck converter (dc/dc converter 2 in Fig. 1), $u_{\rm pv}$ is the control signal (duty cycle), $i_{\rm pv}$ is the current generated by the PV array, n_s is the number of PV cells connected in series, n_p is the number of series strings in parallel, K is the Boltzman constant, A_c is the cell deviation from the ideal $p-n$ junction characteristic, I_{ph} is the photocurrent, and I_{rs} is the reverse saturation current. The power injected by the PV solar module into the dc bus can be computed by

$$P_s = i_s v_b. \tag{6}$$

Note that this power indirectly depends on the control signal $u_{\rm pv}$.

The model of the solar subsystem can be rewritten in the following compact form:

$$\begin{aligned}
\dot{x}_s &= f_s(x_s) + g_s(x_s)u_{\rm pv} \\
h_s(x_s) &= 0
\end{aligned} \tag{7}$$

where $x_s = [v_{\rm pv}\ i_s]^T$ is the state vector of the solar subsystem and $f_s = [f_{s1}\ f_{s2}]^T$, $g_s = [g_{s1}\ g_{s2}]^T$ are nonlinear vector functions and $h_s(x_s)$ is a nonlinear scalar function whose explicit form is omitted for brevity.

The dc bus collects the energy generated by both wind and solar subsystems and delivers it to the load and, if necessary, to the battery bank. The voltage of the dc bus is determined by the battery bank which comprises of lead-acid batteries. The load could be an ac or a dc load. In the case under consideration in the present work, it is assumed to be an ac load; therefore, a voltage inverter is required. We also assume that the future load of the system for certain length of time is known, that is the total power demand is known.

Because all subsystems are linked to the dc bus, their concurrent effects can be easily analyzed by considering their currents in the common dc side. In this way, assuming an ideal voltage inverter, the load current can be referred to the dc side as an output variable current i_L. Therefore, the current across the battery bank can be written as

$$i_b = \frac{\pi}{2\sqrt{3}}\sqrt{i_q^2 + i_d^2}u_w + i_s - i_L \tag{8}$$

where i_L is assumed to be a known current.

The lead-acid battery bank may be modeled as a voltage source E_b connected in series with a resistance R_b and a capacitance C_b. Based on this simple model and (8), the dc bus voltage expression can be written as follows:

$$v_b = E_b + v_c + \left(\frac{\pi}{2\sqrt{3}}\sqrt{i_q^2 + i_d^2}u_w + i_s - i_L\right)R_b \tag{9}$$

where v_c is the voltage in capacitor C_b and its dynamics can be described as follows:

$$\dot{v}_c = \frac{1}{v_b}\left(\frac{\pi}{2\sqrt{3}}\sqrt{i_q^2 + i_d^2}u_w + i_s - i_L\right). \tag{10}$$

The model of the battery bank can also be rewritten in the following compact form:

$$\dot{v}_c = f_c(x_w, x_s, v_c) \tag{11}$$

where $f_c(x_w, x_s, v_c)$ is a nonlinear scalar function.

The dynamics of the hybrid generation system can be written in the following compact form:

$$\dot{x} = f(x) + g(x)u \qquad h(x) = 0 \tag{12}$$

where $x = [x_w^T\ x_s^T\ v_c]$, $u = [u_w\ u_{\rm pv}]$, $f(x)$ and $g(x)$ are suitable composition of f_w, f_s, g_w, g_s and f_c, and $h(x) = h_s(x_s)$. The explicit forms of $f(x)$ and $g(x)$ are omitted for brevity.

Note that the maximum power that can be drawn from the wind and solar subsystems is determined by the maximum power that can be generated by the two subsystems. When the two subsystems are not sufficient to complement the generation to satisfy the load requirements, the battery bank can discharge to provide extra power to satisfy the load requirements. However, when the power limit that can be provided by the battery bank is surpassed, the load must be disconnected to recharge the battery bank and avoid damages. In this work, we do not consider the power needed to charge the battery bank explicitly. However, this power can be lumped into the total power demand. In the reminder of this work, we refer to the total power demand as P_T.

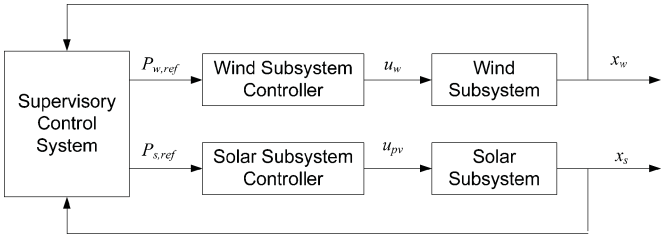

Fig. 2. Supervisory control of a wind-solar hybrid energy system.

III. Control Problem Formulation and Controllers Design

A. Control Problem Formulation

We consider two control objectives of the wind-solar energy generation system. The first and primary control objective is to compute the operating points of the wind subsystem and of the solar subsystem together to generate enough energy to satisfy the load demand. The second control objective is to optimize the operating points to reduce the peak value of surge currents. With respect to the second control objective, specifically, we consider that there are maximum allowable increasing rates of the generated power of the two subsystems and that frequent discharge and charge of the battery bank should be avoided to maximize battery life. Note that the constraints on the maximum increasing rates impose indirect bounds on the peak values of inrush or surge currents to the two subsystems.

The proposed control system is shown in Fig. 2 in which the supervisory control system optimizes the power references $P_{w,\rm ref}$ and $P_{s,\rm ref}$ (operating points) of the wind and solar subsystems, respectively. The two local controllers (wind subsystem controller and the solar subsystem controller) manipulate u_w and $u_{\rm pv}$ to track the power references, respectively.

Remark 1: Note that, in this work, we consider hybrid energy generation systems that already operate in normal generating conditions, and do not address the issues related to system startup or shut down. Moreover, we focus on the application of the proposed supervisory control system and do not provide specific conditions (and detailed theoretical derivation) under which the stability of the closed-loop system is guaranteed. We also note that, in the case of a energy generation system containing several solar and wind subsystems, the proposed supervisory control approach can be extended to control the system in a conceptually straightforward manner by letting the supervisory controller determine the power references of all the subsystems or a distributed MPC approach (in which each MPC controls only some of the subsystems) can be applied. However, the distributed MPC approach is out of the scope of this work.

B. Wind Subsystem Controller Design

For the wind subsystem controller, the objective is to track the power reference computed by the supervisory predictive controller.

In order to proceed, we introduce the maximum power that can be provided by a wind subsystem, $P_{w,\max}$, first. $P_{w,\max}$ depends on a few turbine parameters and on a simple measurement of the angular shaft speed as follows [18]:

$$P_{w,\max} = P_{w,\max}(x) = K_{\rm opt}\omega_m^3 - \frac{3}{2}\left(i_q^2 + i_d^2\right) r_s \qquad (13)$$

where $K_{\rm opt} = (C_t(\lambda_{\rm opt})\rho A R^3)/(2\lambda_{\rm opt}^2)$ and $\lambda_{\rm opt}$ is the tip speed ratio at which the coefficient $C_p(\lambda) = C_t(\lambda)\lambda$ reaches its maximum [18], and $C_t(\cdot)$ is the torque coefficient of the wind turbine.

We follow the controller design proposed in [9]. Specifically, the controller is designed as follows:

$$u_w = \begin{cases} u_{w1}, & \text{if } P_{w,\rm ref} < P_{w,\max} \\ u_{w2}, & \text{if } P_{w,\rm ref} \geq P_{w,\max} \end{cases} \qquad (14)$$

where

$$\begin{aligned} u_{w1} = &-[6r_s(i_q f_{w1} + i_d f_{w2}) - 3\phi_{sr}(\omega_e f_{w1} + i_q f_{w3}) \\ &+ 2(\gamma|s_{w1}(x_w)| + \xi_{\max}|\partial s_{w1}/\partial x_w|) \\ &\times \operatorname{sign}(s_{w1}(x_w))]/(6r_s(i_q g_{w1} + i_d g_{w2}) \\ &- 3\phi_{sr}\omega_e g_{w1}) \\ u_{w2} = &-f_{w1}/g_{w1} + 2K_{\rm opt}\omega_e f_{w3}/(\phi_{sr} g_{w1}) \\ &- i_q f_{w3}/(g_{w1}\omega_e) + 2(\gamma|s_{w2}(x_w)| \\ &+ \xi_{\max}|\partial s_{w2}/\partial x_w|) \times \operatorname{sign}(s_{w2}(x_w))/(3\phi_{sr}\omega_e g_{w1}) \end{aligned}$$

with $\gamma = 1000$ and $\xi_{\max} = 0.02$ being design constants and

$$\left|\frac{\partial s_{w1}}{\partial x_w}\right| = \frac{3}{2}\sqrt{4r_s^2\left(i_q^2 + i_d^2\right) + \phi_{sr}^2\left(\omega_e^2 + i_q^2\right) - 4r_s\phi_{sr}\omega_e i_q}$$

$$\left|\frac{\partial s_{w2}}{\partial x_w}\right| = \sqrt{\left(\frac{3}{2}\phi_{sr}\omega_e\right)^2 + \left(3K_{\rm opt}\omega_e^2 - \frac{3}{2}\phi_{sr} i_q\right)^2}.$$

In the control design shown in (14), $s_{w1} = P_{w\rm ref} - P_w$ and $s_{w2} = P_{w,\max}$ are the sliding surfaces. When the power reference is less than the maximum power that can be provided by the wind subsystem, the control law u_{w1} will operate the subsystem to generate the desired power; when the power reference is greater than the maximum power that can be provided by the wind subsystem, the control law u_{w2} will drive the subsystem to operate at points in which the subsystem provides the maximum power.

C. Solar Subsystem Controller Design

The objective of the solar subsystem controller is to force the subsystem to track the power reference computed by the supervisory controller. The maximum power operating point (MPOP) of the solar subsystem can be computed, in principle, by the following expression [19]:

$$\frac{\partial P_{\rm pv}}{\partial v_{\rm pv}} = \frac{\partial i_{\rm pv}}{\partial v_{\rm pv}} v_{\rm pv} + i_{\rm pv} = 0. \qquad (15)$$

In the present work, the maximum solar power provided, $P_{\rm pv,max}$, is computed numerically through direct evaluation of the following expression [19] in the region where (15) is close to zero

$$P_{\rm pv,max} = P_{\rm pv,max}(x) = -\frac{\partial i_{\rm pv}}{\partial v_{\rm pv}} v_{\rm pv}^2 \cong -\frac{\Delta i_{\rm pv}}{\Delta v_{\rm pv}} v_{\rm pv}^2. \qquad (16)$$

We follow the controller design proposed in [19] to design the solar subsystem controller. Specifically, this controller is designed as follows:

$$\begin{cases} \text{if } P_{\rm pv,max} \geq P_{s,\rm ref} & u_{\rm pv} = \begin{cases} 1, & \text{if } h_1 \geq 0 \\ 0, & \text{if } h_1 < 0 \end{cases} \\ \text{if } P_{\rm pv,max} < P_{s,\rm ref} & u_{\rm pv} = \begin{cases} 0, & \text{if } h_2 \geq 0 \\ 1, & \text{if } h_2 < 0 \end{cases} \end{cases} \qquad (17)$$

where $h_1 = P_{s,\rm ref} - i_s v_b$ and $h_2 = \partial i_{\rm pv}/\partial v_{\rm pv} + i_{\rm pv}/v_{\rm pv}$.

D. Supervisory Controller Design

The objective of the supervisory control system is to determine the power references of the wind and solar subsystems. We propose to design the supervisory controller via MPC. By using MPC, we can take optimality considerations into account as well as handle different kinds of constraints. As stated in Section III-A, the primary control objective is to manipulate the operating points of the wind subsystem and of the solar subsystem together to generate enough energy to satisfy the load demand. This control objective will be considered in the design of the cost function for the MPC optimization problem (please see Section IV). The second control objective is to optimize the operating points to reduce the peak value of surge currents. In order to take into account this control objective, we will incorporate hard constraints in the MPC optimization problem to restrict the maximum increasing rates of the generated power of the two subsystems as well as a term in the cost function to avoid frequent discharge and charge of the battery bank.

We consider the case where the future load of the system for certain length of time is known, that is the total power demand, $P_T(t)$, is known. The main implementation element of supervisory predictive control is that the supervisory controller is evaluated at discrete time instants $t_k = t_0 + k\Delta$, $k = 0, 1, \ldots$, with t_0 the initial time and Δ the sampling time, and the optimal future power references, $P_{w,\rm ref}$ and $P_{s,\rm ref}$, for a time period (prediction horizon) are obtained and only the first part of the references are sent to the local control systems and implemented on the two units. In order to design this controller, first, a proper number of prediction steps N and a sampling time Δ are chosen.

The proposed MPC design for the supervisory control system is described as follows:

$$\min_{P_{w,\rm ref}, P_{s,\rm ref} \in S(\Delta)} \quad \int_{\tau_0}^{\tau_N} L(\tilde{x}(\tau), P_{w,\rm ref}(\tau), P_{s,\rm ref}(\tau))d\tau \qquad (18a)$$

$$\text{s.t.} \quad P_{w,\rm ref}(\tau) \leq \min_{\tau}\{P_{w,\max}(\tau)\}, \quad \tau \in [j\Delta, (j+1)\Delta) \qquad (18b)$$

$$P_{s,\rm ref}(\tau) \leq \min_{\tau}\{P_{\rm pv,max}(\tau)\}, \quad \tau \in [j\Delta, (j+1)\Delta) \qquad (18c)$$

$$P_{w,\mathrm{ref}}((j+1)\Delta) - P_{w,\mathrm{ref}}(j\Delta) \leq dP_{w,\max} \quad (18d)$$

$$P_{s,\mathrm{ref}}((j+1)\Delta) - P_{s,\mathrm{ref}}(j\Delta) \leq dP_{s,\max} \quad (18e)$$

$$\dot{\tilde{x}}(\tau) = f(\tilde{x}(\tau)) + g(\tilde{x}(\tau))u(\tau) \quad (18f)$$

$$h(\tilde{x}) = 0 \quad (18g)$$

$$\tilde{x}(0) = x(t_k) \quad (18h)$$

$$P_{w,\max}(\tau) = P_{w,\max}(\tilde{x}(\tau)) \quad (18i)$$

$$P_{\mathrm{pv},\max}(\tau) = P_{\mathrm{pv},\max}(\tilde{x}(\tau)) \quad (18j)$$

where $\tilde{x}$ is the predicted future state trajectory of the hybrid system, $L(x, P_{w,\mathrm{ref}}, P_{s,\mathrm{ref}})$ is a positive definite function of the state and the two power references that defines the optimization cost, $dP_{w,\max}$ and $dP_{s,\max}$ are the maximum allowable increasing value of $P_{w,\mathrm{ref}}$ and $P_{s,\mathrm{ref}}$ in two consecutive power references, N is the prediction horizon, $j = 0, \ldots, N-1$ and $x(t_k)$ is the state measurement obtained at time t_k. We denote the optimal solution to the optimization problem of (18) as $P^*_{w,\mathrm{ref}}(\tau \,|\, t_k)$ and $P^*_{s,\mathrm{ref}}(\tau \,|\, t_k)$ which are defined for $\tau \in [0, N\Delta)$.

The power references of the two subsystems generated by the supervisory controller of (18) are defined as follows:

$$\begin{aligned} P_{w,\mathrm{ref}}(t) &= P^*_{w,\mathrm{ref}}(t - t_k \,|\, t_k),\ \forall\, t \in [t_k, t_{k+1}) \\ P_{s,\mathrm{ref}}(t) &= P^*_{s,\mathrm{ref}}(t - t_k \,|\, t_k),\ \forall\, t \in [t_k, t_{k+1}). \end{aligned} \quad (19)$$

In the optimization problem of (18), (18a) defines the optimization cost that needs to be minimized, which will be carefully designed in the simulations in Section IV. Because the MPC optimizes the two power references in a discrete time fashion and the references are constants within each sampling interval, the constraints of (18b)–(18c) require that the computed power references should be smaller than the minimal of the maximum available within each sampling interval, which means the power references should be achievable for the wind and solar subsystems. Constraints of (18d)–(18e) impose constraints on the increasing rate of the two power references. In order to estimate the maximum available power of the two subsystems along the prediction horizon, the model of the system (18f), the current state (18g) and the equations expressing the relation between the maximum available power and the state of each subsystem [(18i) and (18j)] are used. Note that in the MPC optimization problem, in order to estimate the future maximum available power of each subsystem, we assume that the environment conditions such as wind speed, insolation and temperature remain constant. When the sampling time is small enough and the prediction horizon is short enough, along with high-frequency wind variations caused by gusts and turbulence being reasonably neglected, this assumption makes physical sense [20]. The constraints of (18b)–(18e) are inspired by results on the design of Lyapunov-based model predictive control systems [24]–[27].

In the remainder of this work, the sampling time and the prediction horizon of the MPC are chosen to be $\Delta = 1$ s and $N = 2$. The maximum increasing values of the two power references are chosen to be $dP_{w,\max} = 1000$ W and $dP_{s,\max} = 500$ W, respectively. Note that the choice of the prediction horizon is based on the fast dynamics of the hybrid generation system, the uncertainty associated with long-term future power demand and is also made to achieve a balance between the evaluation time of the optimization problem of the supervisory MPC and the desired closed-loop performance.

IV. Simulation Results

In this section, we carry out several sets of simulations to demonstrate the effectiveness and applicability of the designed MPC when the control objectives stated in Section III are taken into account. Note that in all the simulations, standard numerical methods, e.g., Runge–Kutta, are used to carry out the numerical integration of the closed-loop system.

A. Constraints on the Maximum Increasing Rates of $P_{w,\mathrm{ref}}$ and $P_{s,\mathrm{ref}}$

In this set of simulations, the control objective is to operate the hybrid wind-solar energy generation system to satisfy the total power demand P_T, subject to constraints on the rate of change of $P_{w,\mathrm{ref}}$ and $P_{s,\mathrm{ref}}$. Because the constraints on the maximum increasing rates of $P_{w,\mathrm{ref}}$ and $P_{s,\mathrm{ref}}$ are considered as hard constraints in the formulation of the MPC [i.e., constraints of (18d)–(18e)], in the cost function, we only penalize the total power demand. The cost function designed for these control objectives is shown as follows:

$$L(x, P_{w,\mathrm{ref}}, P_{s,\mathrm{ref}}) = \alpha(P_T - P_{w,\mathrm{ref}} - P_{s,\mathrm{ref}})^2 + \beta P^2_{s,\mathrm{ref}} \quad (20)$$

where $\alpha = 1$ and $\beta = 0.01$ are constant weighting factors. The first term, $\alpha(P_T - P_{w,\mathrm{ref}} - P_{s,\mathrm{ref}})^2$, in the cost function penalizes the difference between the power generated by the wind-solar system and the total power demand, which drives the wind and solar subsystems to satisfy the total demand to the maximum extent. Because there are infinite combinations of $P_{w,\mathrm{ref}}$ and $P_{s,\mathrm{ref}}$ that can minimize the first term, in order to get a unique solution to the optimization problem, we also put a small penalty on $P_{s,\mathrm{ref}}$. This implies that the wind subsystem is operated as the primary generation system and the solar subsystem is only activated when the wind subsystem alone can not satisfy the power demand. In the simulation, we assume that the environmental conditions remain constant with wind speed $v = 12$ m/s, insolation $\lambda_l = 90$ mW/cm^2 and PV panel temperature $T = 65\,^\circ$C.

Fig. 3 shows the results of the simulations. From Fig. 3, we see that at $t = 4$ s there is a demand power increase from 2100 to 4000 W [see Fig. 3(a)], and that because of the constraints on the maximum increasing rates of $P_{w,\mathrm{ref}}$ and $P_{s,\mathrm{ref}}$, the wind-solar system cannot supply sufficient power [see Fig. 3(b)–(c)] and the shortage of power is made up by the battery bank [see Fig. 3(a)].

Note that we assume that the future power demand for a short time period is known to the MPC. Because of this, at $t = 8$ s, when the MPC supervisory controller receives information about a power demand increase at $t = 9$ s, and having information of the limits on the power generation of the two subsystems, it coordinates the power generations of the wind and solar subsystems to best satisfy the power demand by reducing the power

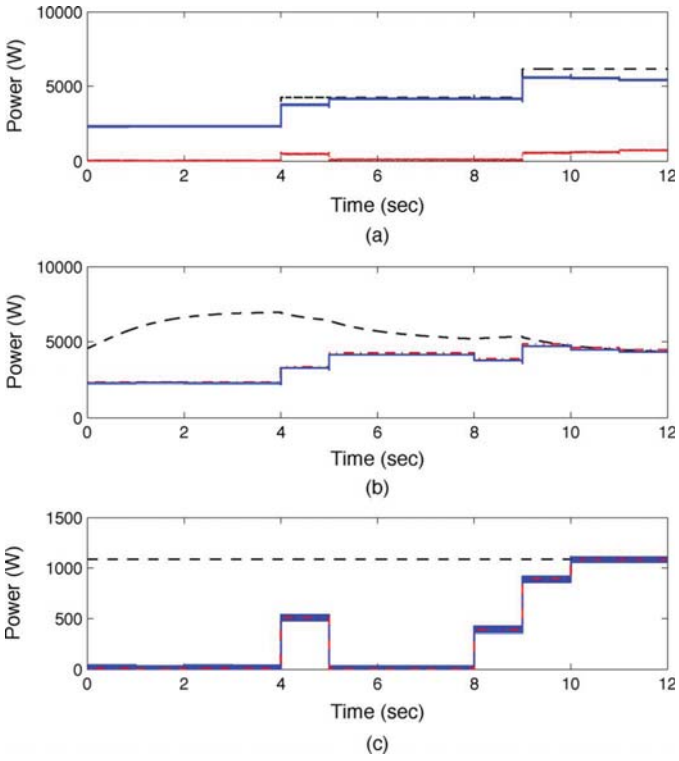

Fig. 3. Power trajectories with constraints on the maximum increasing rates of $P_{w,\mathrm{ref}}$ and $P_{s,\mathrm{ref}}$. (a) Generated power $P_w + P_s$ (solid line), total power demand P_T (dashed line) and power provided by battery bank P_b (dotted line). (b) Power generated by wind subsystem P_w (solid line), wind power reference $P_{w,\mathrm{ref}}$ (dashed-dotted line) and maximum wind generation $P_{w,\max}$ (dashed line). (c) Power generated by solar subsystem P_s (solid line), solar power reference $P_{s,\mathrm{ref}}$ (dashed-dotted line) and maximum solar generation $P_{s,\max}$ (dashed line).

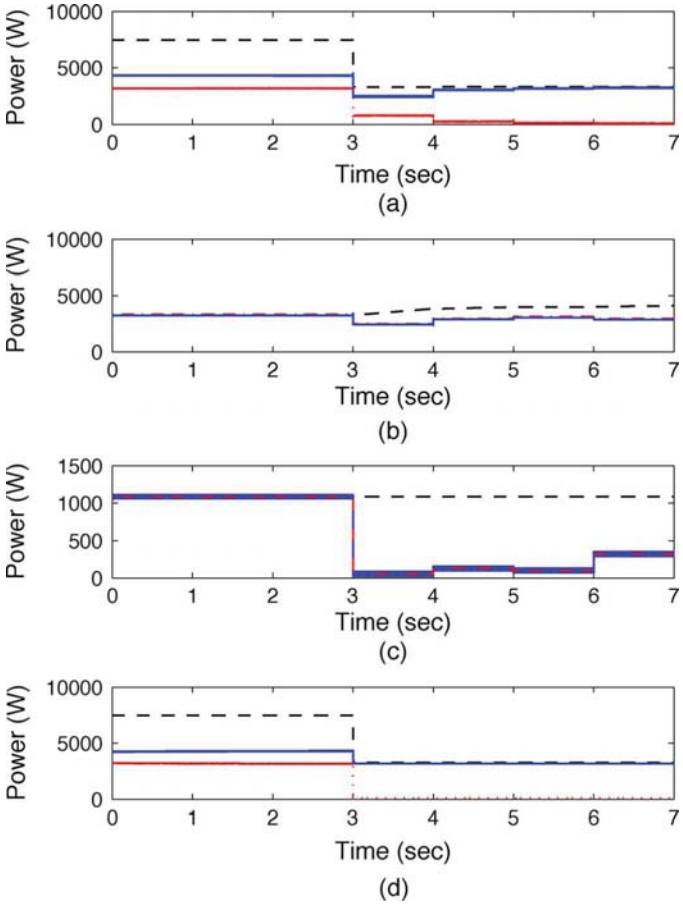

Fig. 4. Power trajectories taking into account suppression of battery power fluctuation. (a) Generated power $P_w + P_s$ (solid line), total power demand P_T (dashed line) and power provide by battery bank P_b (dotted line). (b) Power generated by wind subsystem P_w (solid line), wind power reference $P_{w,\mathrm{ref}}$ (dashed-dotted line) and maximum wind generation $P_{w,\max}$. (c) Power generated by solar subsystem P_s (solid line), solar power reference $P_{s,\mathrm{ref}}$ (dashed-dotted line) and maximum solar generation $P_{s,\max}$. (d) Generated power $P_w + P_s$ (solid line), total power demand P_T (dashed line) and power provide by battery bank P_b (dotted line).

generation of the wind subsystem and activating the solar subsystem in advance at $t = 8$ s. This coordination renders the two subsystems able to approach as much as possible to the total power demand requirement at $t = 9$ s (even though they cannot fully meet this requirement due to operation constraints of the wind and solar subsystems) by boosting their power production at the maximum possible rate, i.e., about 1500 W boost in power production from $t = 8$ s to $t = 9$ s. On the other hand, if there is no information of the future power demand increase that is fed to the MPC, the wind-solar system would not increase its production as fast to approach the total power demand requirement because the solar subsystem would stay dormant up to $t = 9$ s (the power demand requirement at $t = 8$ s can be fully satisfied by the wind subsystem only) and the presence of a hard constraint on the rate of change of power generated by the solar subsystem would not allow to boost its production enough to meet the total power demand requirement at $t = 9$ s (in this case, the total power demand requirement cannot be achieved by operation of the wind subsystem only); as a result the boost in total power production in this case would be only 1200 W.

B. Suppression of Battery Power Fluctuation

In this set of simulations, we modify the cost function of (20) to take into account the fluctuation of the battery power in order to avoid frequent battery charge and discharge. The cost function is modified as follows:

$$L(x, P_{w,ref}, P_{s,ref}) = \alpha(P_T - P_{w,\mathrm{ref}} - P_{s,\mathrm{ref}})^2 + \beta P_{s,\mathrm{ref}}^2 + \zeta \Delta P_b^2 \tag{21}$$

where ΔP_b is the change of the power provided by the battery bank between two consecutive steps and $\zeta = 0.4$ is a weighting factor. Note that this newly added term requires that we store the trajectory of P_b. In this set of simulations, the environmental conditions are set with wind speed $v = 11$ m/s, insolation $\lambda_I = 90$ mW/cm^2 and PV panel temperature $T = 65\,^\circ$C.

Fig. 4 shows the simulation results. From Fig. 4, we see that there is a power demand decrease at $t = 3$ s, and though the wind and solar subsystems are able to provide enough power to satisfy the demand, the supervisory controller will not reduce the power generated by the battery to 0 immediately at $t = 3$ s; instead, the supervisory controller operates the system to make the power provided by the battery bank decrease slower and reach its recharge state at $t = 5$ s [see Fig. 4(a)]. Fig. 4(d)

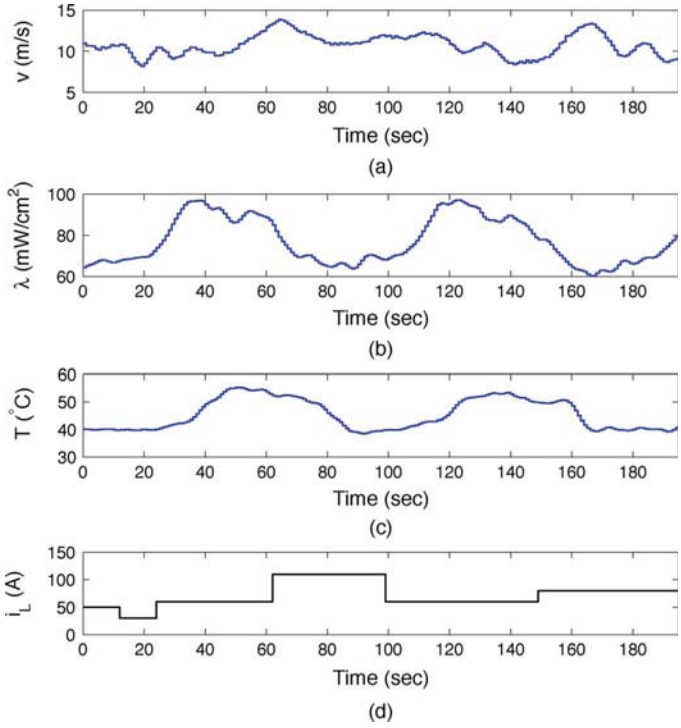

Fig. 5. Environmental conditions and load current. (a) Wind speed v. (b) Insolation λ_l. (c) PV panel temperature T. (d) Load current i_L.

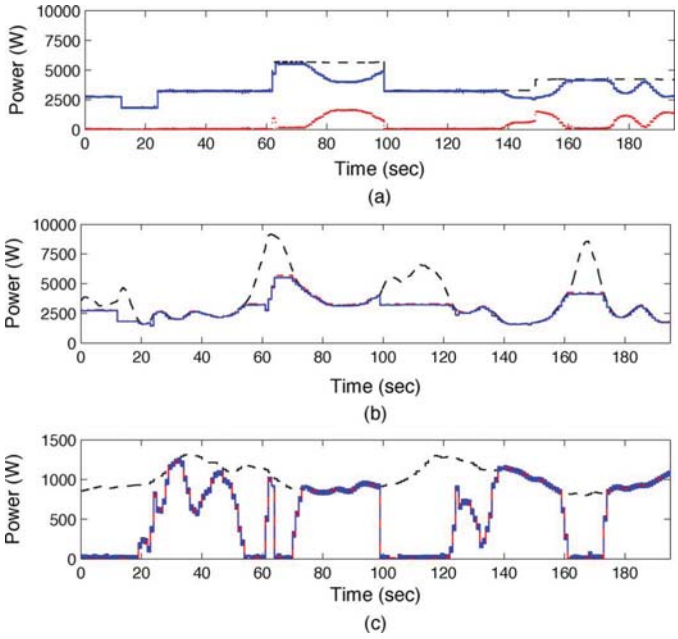

Fig. 6. Power trajectories under varying environment conditions. (a) Generated power $P_w + P_s$ (solid line), total power demand P_T (dashed line), and power provided by battery bank P_b (dotted line). (b) Power generated by wind subsystem P_w (solid line), wind power reference $P_{w,\mathrm{ref}}$ (dashed-dotted line), and maximum wind generation $P_{w,\max}$ (dashed line). (c) Power generated by solar subsystem P_s (solid line), solar power reference $P_{s,\mathrm{ref}}$ (dashed-dotted line), and maximum solar generation $P_{s,\max}$ (dashed line).

shows the power trajectory of the battery bank if no penalty on the change of the power provided by the battery bank is applied.

C. Varying Environmental Conditions

In this subsection, we carry out simulations under varying environmental condition. Time evolution of wind speed, PV panel temperature and insolation are shown in Fig. 5(a)–(c). Fig. 5(d) shows the trajectory of total power demand.

It can be seen from Fig. 6(a) that the wind/solar/battery powers coordinate their behavior to meet the load demand. Time evolution of output power and maximum available power from the wind subsystem and solar subsystem are plotted in Fig. 6(b)–(c). When sufficient energy supply can be extracted from the two subsystems such as during 0–60 s, 100–140 s, and 160–173 s, the battery is being recharged. In other periods, load demand is relatively high and the weather condition, which determines the maximum available generation capacity of the two subsystems, cannot permit sufficient energy supply. Thus, the supervisory controller drives wind/solar parts to their instant maximum capacity and calls the battery bank for shortage compensation.

D. Consideration of High-Frequency Disturbance of Weather Condition

In the preceding scenario, we assumed that the variation of weather-related parameters, like wind speed and insolation, within each sampling time interval is negligible. While this assumption is reasonable in most cases, additional attention for robust system operation should be given under even harsher conditions where high frequency disturbances that influence the values of wind speed and insolation are present. This scenario is possible when the wind turbine encounters turbulent flow [28],

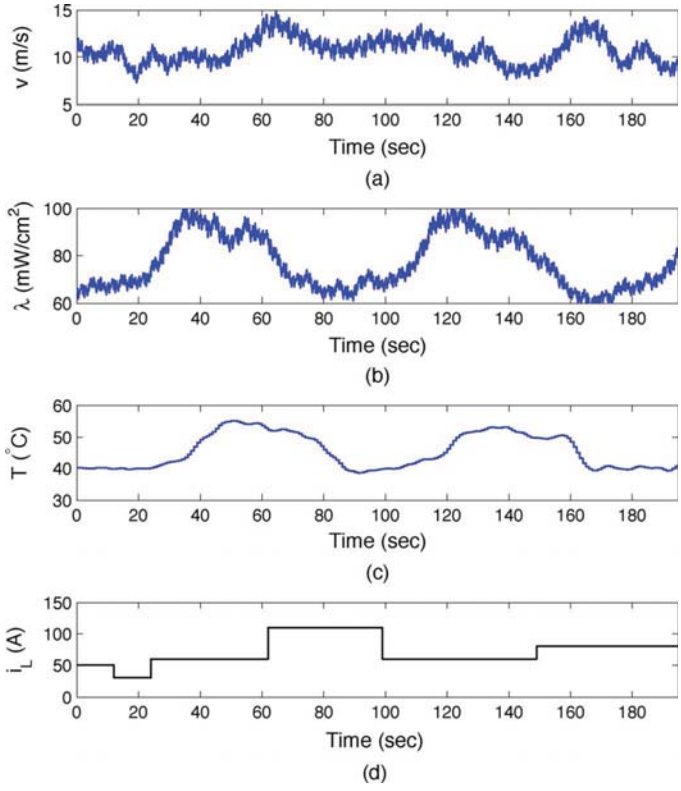

Fig. 7. Environmental conditions and load current. (a) Wind speed with high frequency disturbance v. (b) Insolation with high frequency disturbance λ_l. (c) PV panel temperature T. (d) Load current i_L.

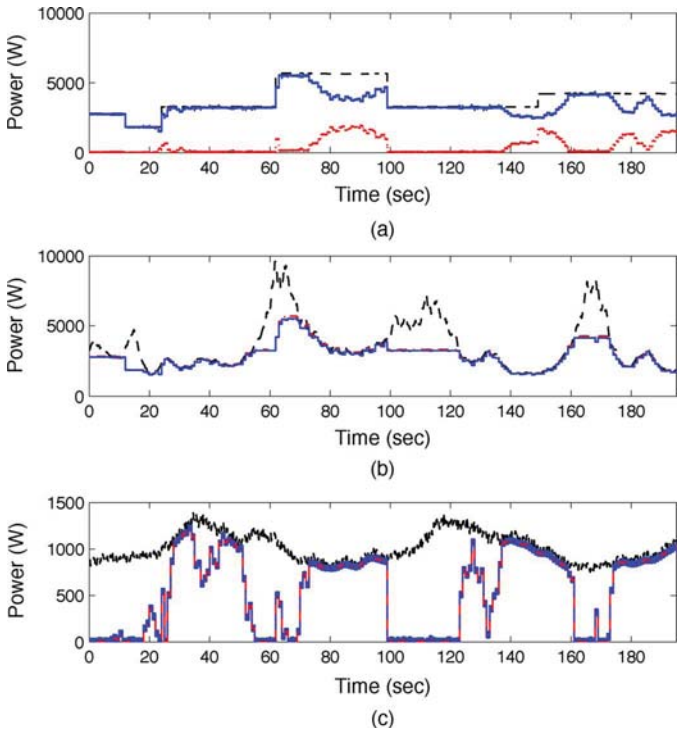

Fig. 8. Power trajectories under varying environment conditions with high frequency disturbance. (a) Generated power $P_w + P_s$ (solid line), total power demand P_T (dashed line), and power provided by battery bank P_b (dotted line). (b) Power generated by wind subsystem P_w (solid line), wind power reference $P_{w,\mathrm{ref}}$ (dashed-dotted line) and maximum wind generation $P_{w,\max}$ (dashed line). (c) Power generated by solar subsystem P_s (solid line), solar power reference $P_{s,\mathrm{ref}}$ (dashed-dotted line) and maximum solar generation $P_{s,\max}$ (dashed line).

or when insolation is affected by abrupt changes in atmospheric turbidity [29].

To study this case from a control point of view and evaluate the robustness of the proposed control system in this case, we introduce disturbances in two parameters; specifically, 10% variation in the wind speed and 5% variation in the insolation. The profiles of the wind speed and insolation are shown in Fig. 7(a) and (b). We have used the system model to establish that the control system operating on the wind subsystem can tolerate the wind disturbance and no additional measures are needed to be taken to secure its reliability. However, for the solar subsystem, which is characterized by faster dynamics, in order to maintain its closed-loop stability we need to use a more conservative estimate of the insolation (i.e., 95% of the value of the measured insolation) in the evaluation of the power reference. This conservative estimate of insolation ensures that the predicted maximum power delivered by the solar subsystem does not exceed what the weather permits.

The closed-loop profiles of power generation are displayed in Fig. 8(a)–(c). Again, the entire energy generation system operates reliably, thereby yielding positive results for the robustness of the control system with respect to abrupt variations in wind speed and insolation. Both maximum power generation capabilities of the two subsystems are perturbed as a result of the weather disturbance, but both the wind subsystem and the solar subsystem operate in a robust fashion and the total power demand is met.

V. Conclusion

In this work, we focused on the development of a supervisory predictive control method for the optimal management and operation of hybrid wind-solar energy generation systems. We proposed a supervisory control system designed via MPC which computes the power references for the wind and solar subsystems at each sampling time while minimizing a suitable cost function. The power references are sent to two local controllers which drive the two subsystems to the power references. We discussed how to incorporate practical considerations, for example, how to reduce the peak values of inrush or surge currents, into the formulation of the MPC optimization problem. Simulation results demonstrated the effectiveness and applicability of the proposed approach. Future work will include the investigation of large time span behavior of the hybrid wind-solar generation system taking into account information of future weather forecast, and investigation of the performance of the system under the condition that the future power demand is unknown.

References

[1] California Energy Commission, "2008 energy policy report update," 2008.
[2] R. Spee and J. H. Enslin, "Novel control strategies for variable-speed doubly fed wind power generation systems," *Renewable Energy*, vol. 6, pp. 907–915, 1995.
[3] P. Novak, T. Ekelund, Y. Jovik, and B. Schmidtbauer, "Modeling and control of variable-speed wind-turbine drive system dynamics," *IEEE Control Syst. Mag.*, vol. 15, no. 4, pp. 28–37, Aug. 1995.
[4] T. Thiringer and J. Linders, "Control by variable rotor speed of fixed-pitch wind turbine operating in speed range," *IEEE Trans. Energy Conv.*, vol. 8, no. 3, pp. 520–526, Sep. 1993.
[5] M. G. Simoes, B. K. Bose, and R. J. Spiegel, "Fuzzy logic based intelligent control of a variable speed cage machine wind generation system," *IEEE Trans. Power Electron.*, vol. 12, no. 1, pp. 87–95, Jan. 1997.
[6] K. Uhlen, B. A. Foss, and O. B. Gjosaeter, "Robust control and analysis of a wind-diesel hybrid power plant," *IEEE Trans. Energy Conv.*, vol. 9, no. 4, pp. 701–708, Dec. 1994.
[7] F. Valenciaga, P. F. Puleston, R. J. Mantz, and P. E. Battaiotto, "An adaptive feedback linearization strategy for variable speed wind energy conversion systems," *Int. J. Energy Res.*, vol. 24, pp. 151–161, 2000.
[8] K. Tan and S. Islam, "Optimum control strategies in energy conversion of PMSG wind turbine system without mechanical sensors," *IEEE Trans. Energy Conv.*, vol. 19, no. 2, pp. 392–399, Jun. 2004.
[9] F. Valenciaga, P. F. Puleston, and P. E. Battaiotto, "Variable structure system control design method based on a differential geometric approach: Application to a wind energy conversion subsystem," *IEE Proc.—Control Theory Appl.*, vol. 151, pp. 6–12, 2004.
[10] M. Chinchilla, S. Arnaltes, and J. C. Burgos, "Control of permanent-magnet genrators applied to variable-speed wind energy systems connected to the grid," *IEEE Trans. Energy Conv.*, vol. 21, no. 1, pp. 130–135, Mar. 2006.
[11] F. Valenciaga and P. F. Puleston, "High-order sliding control for a wind energy conversion system based on a permanent magnet synchronous generator," *IEEE Trans. Energy Conv.*, vol. 23, no. 3, pp. 860–867, Sep. 2008.
[12] D. Q. Dang, Y. Wang, and W. Cai, "Nonlinear model predictive control (NMPC) of fixed pitch variable speed wind turbine," in *Proc. IEEE Int. Conf. Sustainable Energy Technol.*, Singapore, 2008, pp. 29–33.
[13] T. A. Johansen and C. Storaa, "Energy-based control of a distributed solar collector field," *Automatica*, vol. 38, pp. 1191–1199, 2002.
[14] F. Coito, J. M. Lemos, R. N. Silva, and E. Mosca, "Adaptive control of a solar energy plant: Exploiting accessible disturbances," *Int. J. Adapt. Control Signal Process.*, vol. 11, pp. 327–342, 1997.
[15] E. F. Camacho and M. Berenguel, "Robust adaptive model predictive control of a solar plant with bounded uncertainties," *Int. J. Adapt. Control Signal Process.*, vol. 11, pp. 311–325, 1997.
[16] N. Hamrouni, M. Jraidi, and A. Cherif, "New control strategy for 2-stage grid-connected photovoltaic power system," *Renewable Energy*, vol. 33, pp. 2212–2221, 2008.

[17] T. Yoshida, K. Ohniwa, and O. Miyashita, "Simple control of photovoltaic generator systems with high-speed maximum power point tracking operation," *EPE J.*, vol. 17, pp. 38–42, 2007.
[18] F. Valenciaga, P. F. Puleston, P. E. Battaiotto, and R. J. Mantz, "Passivity/sliding mode control of a stand-alone hybrid generation system," *IEE Proc.—Control Theory Appl.*, vol. 147, pp. 680–686, 2000.
[19] F. Valenciaga, P. F. Puleston, and P. E. Battaiotto, "Power control of a photovoltaic array in a hybrid electric generation system using sliding mode techniques," *IEE Proc.—Control Theory Appl.*, vol. 148, pp. 448–455, 2001.
[20] F. Valenciaga and P. F. Puleston, "Supervisor control for a stand-alone hybrid generation system using wind and photovoltaic energy," *IEEE Trans. Energy Conv.*, vol. 20, no. 2, pp. 398–405, Jun. 2005.
[21] N. A. Ahmed, M. Miyatake, and A. K. Al-Othman, "Hybrid solar photovoltaic/wind turbine energy generation system with voltage-based maximum power point tracking," *Electric Power Components Syst.*, vol. 37, pp. 43–60, 2009.
[22] C. E. García, D. M. Prett, and M. Morari, "Model predictive control: Theory and practice—A survey," *Automatica*, vol. 25, pp. 335–348, 1989.
[23] J. B. Rawlings, "Tutorial overview of model predictive control," *IEEE Control Syst. Mag.*, vol. 20, no. 3, pp. 38–52, Jun. 2000.
[24] P. D. Christofides and N. H. El-Farra, *Control of Nonlinear and Hybrid Process Systems: Designs for Uncertainty, Constraints and Time-Delays.*. New York: Springer, 2005.
[25] P. Mhaskar, N. H. El-Farra, and P. D. Christofides, "Stabilization of nonlinear systems with state and control constraints using Lyapunov-based predictive control," *Syst. Control Lett.*, vol. 55, pp. 650–659, 2006.
[26] P. Mhaskar, N. H. El-Farra, and P. D. Christofides, "Predictive control of switched nonlinear systems with scheduled mode transitions," *IEEE Trans. Autom. Control*, vol. 50, no. 11, pp. 1670–1680, Nov. 2005.
[27] D. Muñoz de la Peña and P. D. Christofides, "Lyapunov-based model predictive control of nonlinear systems subject to data losses," *IEEE Trans. Autom. Control*, vol. 53, no. 9, pp. 2076–2089, Oct. 2008.
[28] J. Peinke, E. Anahua, St. Barth, H. Goniter, A. P. Schaffarczyk, D. Kleinhans, and R. Friedrich, "Turbulence a challenging issue for the wind energy conversion," presented at the Eur. Wind Energy Conf. Exhibition, Brussels, Belgium, 2008.
[29] J. Hofierka and M. Suri, "The solar radiation model for open source GIS: Implementation and applications," in *Proc. Open Source GIS—GRASS Users Conf.*, Trento, Italy, 2002, pp. 1–19.

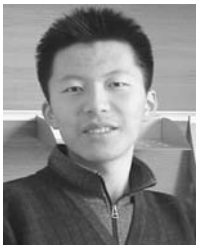

Wei Qi was born in Gansu, China, in 1988. He is currently pursuing the B.S. degree in control science and engineering from Zhejiang University, Zhejiang, China.

In the summer of 2009, he was a Research Student with the group of Prof. Christofides at University of California, Los Angeles. His research interests mainly focus on model predictive control.

Jinfeng Liu was born in Wuhan, China, in 1982. He received the B.S. and M.S. degrees in control science and engineering from Zhejiang University, China, in 2003 and 2006, respectively. He is currently pursuing the Ph.D. degree in chemical engineering from the University of California, Los Angeles.

His research interests include model predictive control, fault detection and isolation, and fault-tolerant control of nonlinear systems.

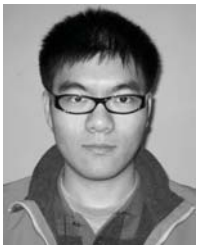

Xianzhong Chen was born in Guangzhou, China, in 1985. He received the B.S. and M.S. degrees from the Department of Chemical and Biomolecular Engineering, University of California, Los Angeles, in 2008 and 2010, respectively, where he is currently pursing the Ph.D. degree.

His research interests include model predictive control and process control.

Panagiotis D. Christofides (M'02–SM'07–F'09) was born in Athens, Greece, in 1970. He received the Diploma in chemical engineering from the University of Patras, Patras, Greece, in 1992, the M.S. degrees in electrical engineering and mathematics and the Ph.D. degree in chemical engineering from the University of Minnesota, Minneapolis, in 1995, 1996, and 1996, respectively.

Since July 1996, he has been with the University of California, Los Angeles, where he is currently a Professor with the Department of Chemical and Biomolecular Engineering and the Department of Electrical Engineering. A description of his research interests, list of distinctions and a list of his publications can be found at http://www.chemeng.ucla.edu/pchristo/index.html.